We are IntechOpen,
the world's leading publisher of
Open Access books
Built by scientists, for scientists

6,900
Open access books available

186,000
International authors and editors

200M
Downloads

Our authors are among the

154
Countries delivered to

TOP 1%
most cited scientists

12.2%
Contributors from top 500 universities

CLARIVATE ANALYTICS
BOOK CITATION INDEX
INDEXED

WEB OF SCIENCE™

Selection of our books indexed in the Book Citation Index
in Web of Science™ Core Collection (BKCI)

Interested in publishing with us?
Contact book.department@intechopen.com

Numbers displayed above are based on latest data collected.
For more information visit www.intechopen.com

From 11% Thin Film to 23% Heterojunction Technology (HJT) PV Cell: Research, Development and Implementation Related 1600 × 1000 mm² PV Modules in Industrial Production

Eugenii Terukov, Andrey Kosarev,
Alexey Abramov and Eugenia Malchukova

Additional information is available at the end of the chapter

Abstract

Plasma-enhanced chemical vapor deposition (PECVD) developed for thin film (TF) Si:H-based materials resulted in large area thin film PV cells on glass and flexible substrates. However, these TF cells demonstrate low power conversion efficiency PCE = 11% for double and PCE = 13% for triple junction cells below predicted PCE ≈ 24%. PV cells on crystalline silicon (c-Si) provide PCE ≈ 17–19%. Cost of c-Si PV cells lowered continuously due to reducing price of silicon wafers and enlarging their size. Two factors stimulated a combination of PECVD films and c-Si devices: (a) compatibility of the technologies and (b) possibility for variation of electronic properties in PECVD materials. The latter results in additional build-in electric fields improving charge collection and harvesting solar spectrum. We describe a transformation of PECVD TF solar cell technology for 11% efficiency modules to heterojunction technology (HJT) c-Si modules with 23% efficiency. HJT PV structure comprises c-Si wafer with additional junctions created by PECVD deposited layers allowing development of single wafer PV cells with PCE ≈ 24% and the size limited by wafer (15.6 x 15.6 cm²). The chapter starts with background in PECVD and c-Si PV cells. Then, in Section 2, we describe electronic properties of PECVD materials in HJT PV structures. Section 3 deals with structure and fabrication process for HJT devices. In Section 4, we present and discuss performance characteristics of the devices. Section 5 describes implementation of the developed HJT module (1600 x 1000 mm²) based on HJT single wafer cells in industry with presentation and discussion of characteristics related to industrial production. Finally, Section 6 presents the outlook and summary of the chapter.

Keywords: photovoltaic solar cells, HJT silicon solar cells, solar cell modules, plasma deposition

1. Introduction

Market of PV devices shows continuous increase, for example, for only 1 year, that is, 2016–2017, it has grown from 76 GW to about 100 GW (by more than 30%) [1]. PV devices based on silicon dominate in the market (>90%). Interdigitated back contact (IBC) cells on monocrystalline n-type silicon demonstrate mass production efficiency, PCE = 23% (2016) with prognosis to rise to PCE = 27% by 2027 [1]. Fabrication of these devices is complicated because of multiple deposition and etching steps required to form both p- and n-doped contact areas on rear surface of the cells. Moreover this fabrication is based on conventional crystalline silicon technology including high temperature processes. Alternative and relatively simple approach to get high efficiency defined as heterojunction technology (HJT) includes deposition of thin layers by plasma-enhanced chemical vapor deposition (PECVD) conducted at low temperature. PECVD technique provides a wide range of possibilities for material engineering with variation of structure, electronic properties and doping of the films. These films can be used for surface passivation and for creation of additional built in electric field at interfaces with silicon. HJT solar cells exhibit PCE = 22% (2016) with prognosis for rise to PCE = 24% in 2027 [1]. Furthermore, a combination of HJT and back contact technology will allow to overcome PCE values predicted for conventional IBC cells made with diffusion approach as it is confirmed by a world record PCE values above 26% reported for such cells [2].

PECVD is a rather mature industrial technology exploited to fabricate both PV modules on both glass substrate with dimensions up to 2200 × 2600 mm^2 and flexible plastic or metal foil substrates. The best developed PECVD PV structures provide efficiency, that is, PCE = 11% for "micromorph" two junction tandem [3] and PCE = 13% for triple tandem on stainless steel foil [4]. These values are less than those theoretically predicted PCE = 24%. Therefore, PECVD PV solar cell modules on glass are not able to compete with those based on crystalline silicon technology for terrestrial applications, though they occupy a segment of flexible solar cells in PV market. Advantages of PECVD technology for material engineering together with compatibility of this technique with c-Si technology made promising implementation of PECVD materials in c-Si PV technology resulting in development of HJT solar cells. The latter is attractive because of PECVD is a low-temperature process and also because of its performance demonstrated.

This chapter describes our experience in research and development of HJT solar cells and modules based on our previous background in fabrication of "micromorph" modules; implementation of HJT modules consisted of 60 cells in industrial production is also discussed.

2. Configurations and fabrication of HJT devices

In this section, we describe basic configurations of solar cells based on crystalline materials. **Figure 1** shows cross-section diagrams for crystalline silicon solar cell (a) fabricated by standard

diffusion processes with typical efficiency of 17–19%, PECVD thin silicon film "tandem" structure (c) comprising two p-i-n junctions with efficiency of 9–11% and HJT silicon-based solar cell incorporating some PECVD films.

n-Type c-Si is a conventional material for HJT cells nowadays, although HJT solar cells based on p-type silicon with efficiency above 20% have been also reported, for example, see Ref. [5].

Despite using floating zone (FZ), c-Si for record cells and reasonable parameters obtained on high-quality multicrystalline wafers manufactured with direct solidification technique [6], crystalline silicon made by Czochralski (CZ) technique is conventionally used for HJT cells' mass production. In this study, 6" CZ Si pseudo square n-doped <100> wafers with typical resistivity in the range from 1 to 5 Ohm·cm were used. The wafers were sliced with diamond wire technology from ingots with low impurity level providing bulk lifetime of minority carriers τ > 1 ms measured by transient photoconductance technique on ingots.

It is worthy of some comments in terms of different HJT configurations. Frontal side of solar cell is determined as that for penetration of incident light, and opposite side is determined as rare (or back) side. There is also not well-justified term "emitter" which nevertheless is widely used in the literature, it is referred to the position of p(or p$^+$) layer. Two configurations of HJT cells are possible: with frontal emitter meaning p-layer position on frontal side and rare (back) emitter meaning p-layer on rear side. For industrial production, to our mind rear emitter is preferable because of higher contribution of the wafer in lateral conductivity resulting in lower requirements for contact grid (lines may be narrower and separated by longer distance) and consequently, reducing shadow losses. In addition, employing n-layer made of nanocrystalline silicon (PECVD nc-Si) on frontal side results in reducing absorption losses from frontal side. However, lower holes diffusion length and nonuniform absorption of the incident light inside of c-Si wafer resulting in much higher carrier generation rate at
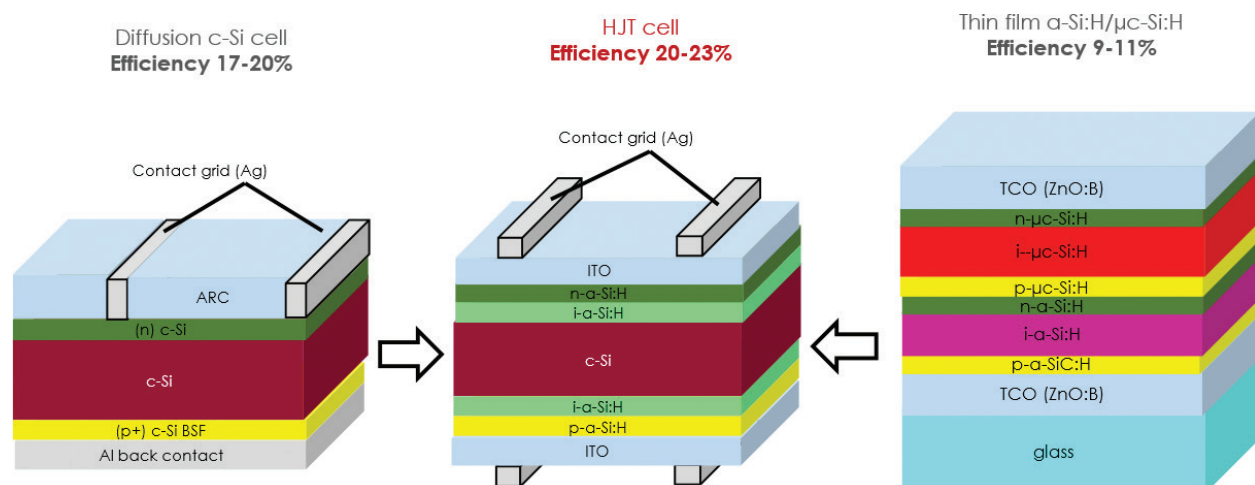

Figure 1. Configurations of different solar cells: (a) crystalline silicon c-Si device fabricated with diffusion processes, (b) HJT cell comprising c-Si and PECVD materials and (c) thin film a-Si:H/mk-Si:H solar cell (two junction tandem).

front interface lead to record efficiencies on laboratory cells with frontal emitter configuration [7]. As seen in **Figure 1(b)** and **(c)**, the structures comprise different PECVD films such as un-doped (e.g., amorphous silicon a-Si:H, microcrystalline mk-Si:H), p-doped (e.g. p-a-SiC:H, p-mk-Si:H) and n-doped (e.g. n-a-Si:H, n-mk-Si:H). Electronic properties of these films are discussed in Section 3 and film deposition in Section 5.

Here, we would like to provide some comments on functions of these films in device structures. Historically, first c-Si solar cells contained p- and/or n-doped layers prepared with diffusion, and they contacted to metals. They are characterized by significant losses at interfaces due to several processes, for example, free carrier absorption, surface recombination, and so on, and efficiency achieved is 17–19%. Further progress is related to the development of significantly more complex structures such as passivated emitter rear locally diffused (PERL) [8] and passivated emitter and rear cell (PERC) solar cells [9]. Then PV structures prepared by heterojunction technology called HJT solar cells_ have been developed [9]. In these HJT structures crystalline silicon surfaces is passivated by PECVD films which also create heterojunctions providing additional built-in electric fields, reduce surface recombination and back diffusion of photocarriers and serve as anti-epitaxial buffer.

3. Electronic properties of PECVD materials used in HJT solar cells

Let us consider some principal electronic properties of PECVD films used in HJT solar cells. They are listed in **Table 1** that contains some electrical and optical characteristics of the films. It is seen that properties of PECVD films differ significantly from those in crystalline materials comprising the same atoms. For example, optical gap for c-Si Eg = 1.1 eV and for amorphous silicon a-Si:H Eg = 1.62–1.65 eV, there is also a difference in activation energy of conductivity. These films can be also doped in n- and p-type though with less efficiency of doping compared to crystalline one. Difference of these characteristics provides possibility creation of heterojunctions with crystalline silicon resulting in local built-in electric fields. Conventionally, PECVD films are deposited from hydride gases such as silane (SiH_4), methane (CH_4), and

Layer type	E_g (eV)	n@500 nm	k@500 nm	E_a (eV)
i-layer(a-Si:H)[*]	1.65	4.79	0.61	0.75–0.82
p-layer(a-Si:H)	1.62	4.2	0.47	0.3–0.4
n-layer(a-Si:H)	1.63	4.72	0.6	0.25–0.35
p-layer (nc-Si:H)	1.87[*]	4.22	0.18	0.08–0.12
n-layer (nc-Si:H)	1.83[*]	4.16	0.20	0.02–0.04
p-layer (a-SiC:H)	2.02	3.49	0,24	0.45–0.50

[*]E^{04} values are presented.

Table 1. Electronic properties of PECVD films incorporated in HJT solar cells.

germane (GeH_4), which are often supplied as a mixture with hydrogen. Thus, glow discharge during film growth contains significant amount of hydrogen in the form of molecules, atoms and ions. The latter two are very active chemically promoting passivation of substrate surface, which is of principle importance during fabrication of HJT solar cells.

There are various techniques to grow thin device quality films, for example, atomic layer deposition (ALD), hot wire (HW) deposition, inductively coupled plasma (ICP), direct current (DC), low frequency (LF), radio frequency (RF), very high frequency (VHF), microwave plasma in capacitance type reactors, and so on. Comparison of these techniques is out of the scope of the chapter; therefore, we only notice that the industry is mostly employed with RF and VHF PECVD systems. The latter type is used for fabrication of HJT solar cells in this chapter.

Nanometer-scale thicknesses of the PECVD films in HJT structures are really a challenge in material engineering and electronic characterization of such films. Conventionally, at initial stage, material of each film and its electronic properties are optimized by preparing the samples on appropriate substrate such as glass or silicon. Thickness of the film at this stage is more than 100 nm, while in HJT structures, we need 5–20 nm thickness. Therefore, questions arise: is it possible to characterize such thin films? Is it possible to apply electronic characteristics measured in thicker films in device design? Up to now, there are contradictory data reported. Some researchers have observed changes in electronic properties with thickness [10], while others have revealed such behavior. Here, we present some data obtained in thin films by attenuated total reflection infrared spectroscopy (ATR IR) spectroscopy technique allowing characterization of rather thin films. To our mind, both spectral ellipsometry and ATR IR are widely used technique for thin film characterization. ATR IR spectroscopy allows measurements of the films with thickness less than 20 nm, that is, in the range of thickness of the films in HJT device structures. **Figure 2** shows IR spectra (measured by transmission on silicon substrate and ATR IR technique) of the films deposited on different substrate (glass and silicon) in the same run. The peaks for both curves are located at the value of k = 2000 cm^{-1} suggesting practically the same hydrogen bonding structure in the samples.

Figure 3 presents ATR IR spectra around k = 2000 cm^{-1} (Si-H stretching mode) for the intrinsic and doped samples with different thicknesses. One can see in the figure that using ATR IR absorption spectra of a-Si:H film, it is possible to observe Si-H stretching mode in the films with thickness less than 20 nm; therefore, this technique can be effectively used for optimization of the films with thickness required for HJT cells. It is clearly seen that all the curves are well centered at k = 2000 cm^1. No detectable changes have been observed with thickness.

This is revealed even more clearly in **Figure 4**, where the spectra are normalized at maximum value for both intrinsic and p-doped layer. Thus, we have demonstrated some evidence for negligible effect of thickness on microstructure and consequently on electronic properties.

In other words, some basic material optimization can be performed by optical measurements with ellipsometry or ATR IR spectroscopy in the films deposited on some acceptable substrates (e.g., on glass), which is of principal importance for optimization of uniformity and electronic properties in ultrathin films deposited in mass production PECVD systems.
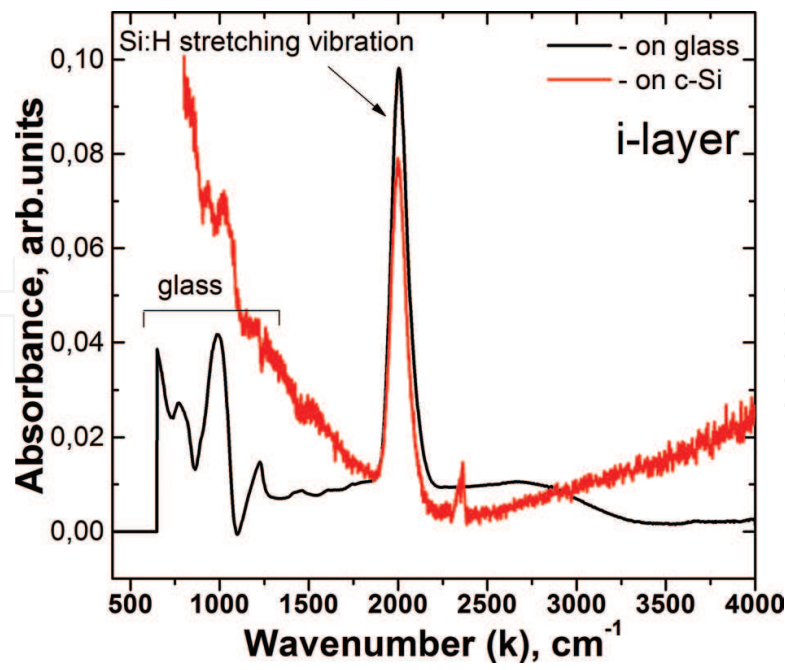
Figure 2. IR absorption spectra measured by transmission and ATR IR spectroscopy.

After the basic optimization, the characteristics obtained can be extrapolated to the thicknesses of the films in device structures. However, such optimization is only initial stage because always growth conditions for the films even in the same run (with fixed operator deposition parameters) are different for the film deposited on glass from those when the film is deposited on stack of previously deposited films. Therefore, it should be noted that final optimization of the films is performed in concrete device structures for concrete film inserted between other materials. Figures of merit for such optimization are performance characteristics of the device.
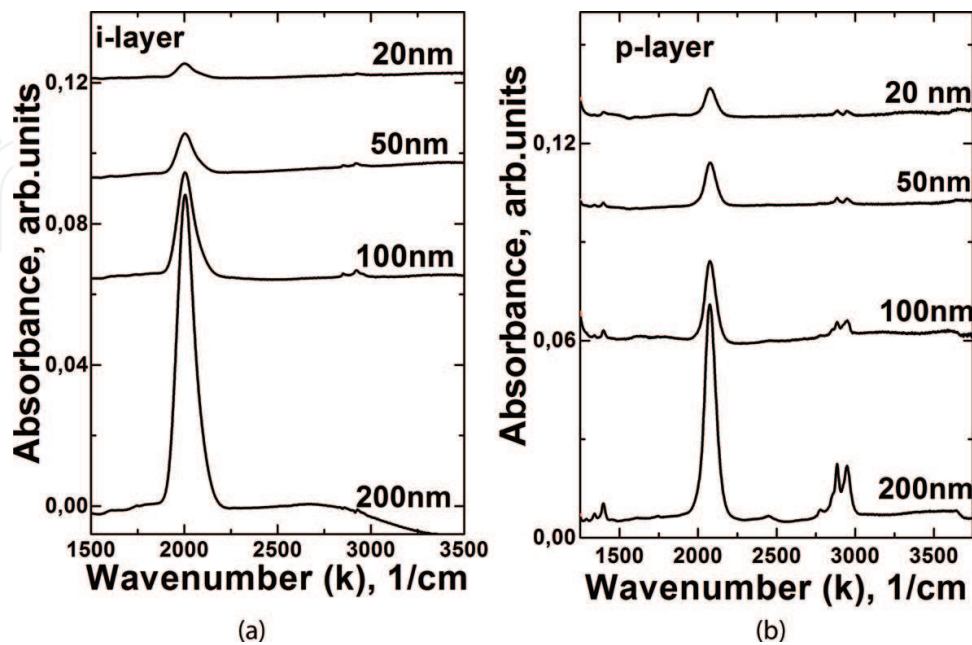

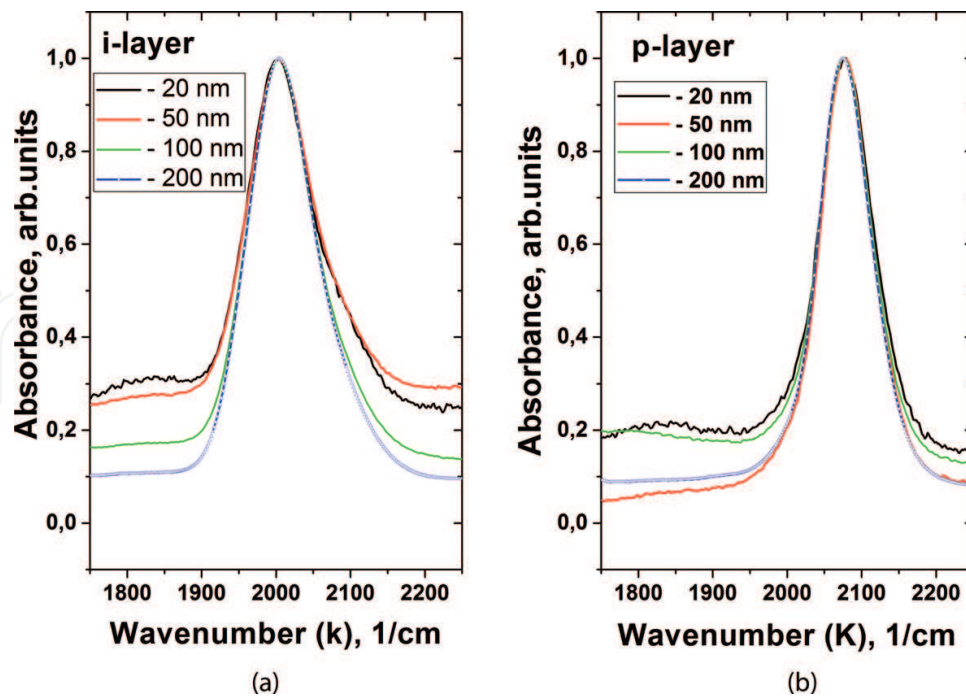**Figure 3.** ATR IR spectra of intrinsic (a) and doped (b) a-Si:H layers of different thickness.

Figure 4. Normalized IR absorbance spectra for intrinsic i-a-Si:H (a) and p-doped p-Si:H layers (b).

4. Performance characteristics of HJT solar cells (single wafer devices)

Performance characteristics of both solar cells and modules allow obtaining finally power conversion efficiency (PCE) of solar energy into electric energy, to see harvesting photons of different energy of the Sun spectrum and to get insight into technological issues. In this section, we describe and discuss these characteristics for single wafer HJT solar cells.

PCE values are conventionally determined from current–voltage J(U) characteristics measured with illumination of solar simulator providing incident light intensity $I_{inc} = 1000$ W/m^2 and AM 1.5 conditions. An example of J(U) characteristic is shown in **Figure 7**, and the characteristics calculated from this J(U) curve are given in the insert. PCE is defined by the following equation:

$$PCE = \eta = \left(J_{sc}\, U_{oc}\right) FF/I_{inc} \qquad (1)$$

where J_{sc} is the short circuit current density determined at U = 0, U_{oc} is the open circuit voltage determined at J = 0, I_{inc} is the incident light intensity and FF is the fill factor.

Progress in efficiency for single wafer HJT solar cells and some images of the samples as a function of R&D time in RDC TF TE are presented in **Figure 5**.

Starting in 2014, with small area prototypes RDC TF TE in 2017 achieved PCE = 22.8% for solar cell with 156 × 156 mm^2 dimensions (corresponding area S = 244 cm^2) in 2017. This cell is the base for large area modules with dimensions 1600 × 1000 mm^2. Fabrication and characteristics of this module are presented and discussed in Section 5.
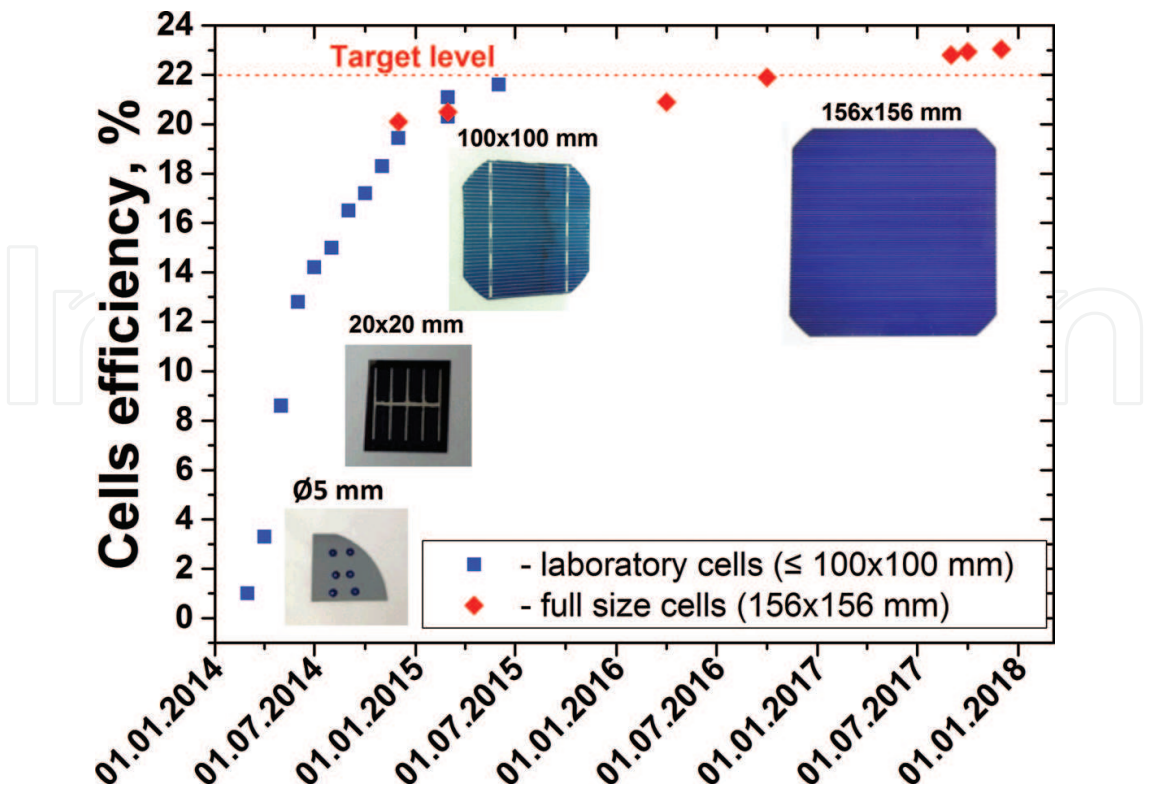
Figure 5. PCE increase of HJT single wafer solar cell during the development in RDC TF TE.

In order to improve light trapping in the device structures, Si wafers were textured using isopropanol alcohol (IPA) free alkaline process. Despite diamond wire, sliced wafer can be successfully textured from as cut state without surface damage etch (SDE) step, we used SDE because it facilitated uniform texturing, improved process stability and reduced production costs by lower consumption of surfactants providing anisotropic Si etching along <111> direction.
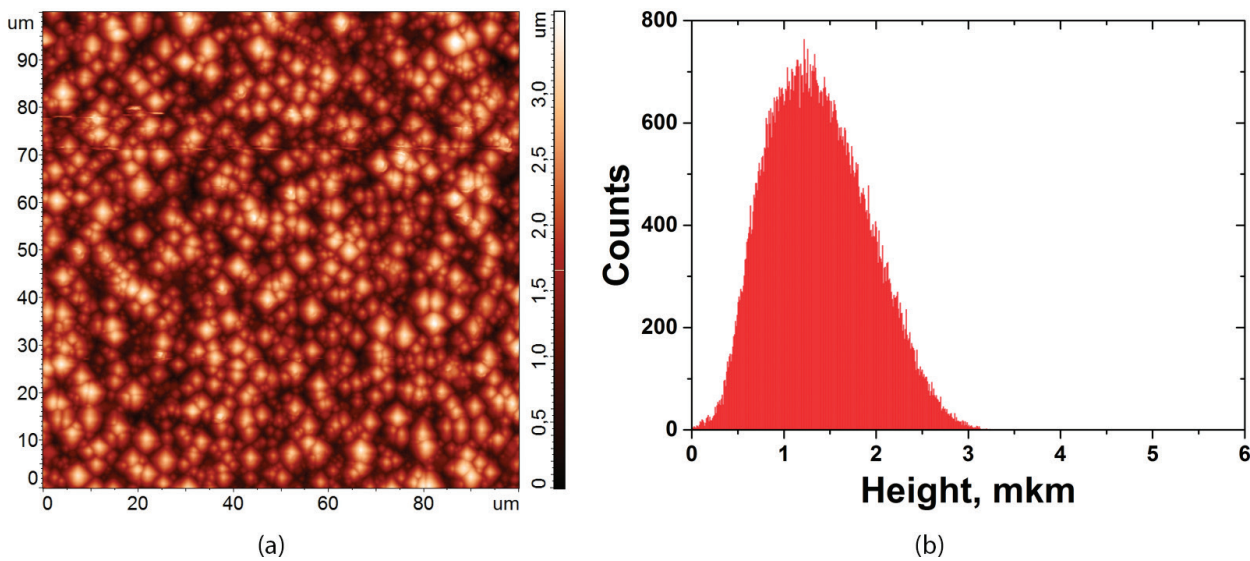

Figure 6. AFM image of textured Si wafer surface (a) and distribution function of heights (b).

As a consequence, textured wafers have pyramidal surface topology with size and distribution of pyramids controlled by parameters of etching process. An example of AFM image of textured wafer is shown in **Figure 6**. One can see in the figure that surface of textured wafer is uniformly covered by pyramids with average height about 1.5 mkm.

Special attention has been paid to final cleaning of wafers surface from organic and metal impurities. We used several cleaning steps followed by final HF-dip and hot nitrogen drying procedure.

Current-voltage characteristic of our best cell measured under standard test conditions (STC) is shown in **Figure 7** for single wafer HJT solar cell (156 × 156 mm^2). This cell exhibits such parameters as efficiency PCE = 23.04%, Uoc = 735 mV, Isc = 9.45 A and FF = 81.0%.

Spectral characteristics for different c-Si solar cells, including single wafer HJT solar cell, are presented in **Figure 8**. Comparing spectral curves in **Figure 8**, we can see that PERC solar cell has higher response in short wavelength range (λ < 500 nm) and lower response in long wavelength region (λ > 900 nm) than HJT device resulting in a small difference about 2% in integral current. Multicrystalline solar cell made by the BSF technology currently dominating in PV market has a little bit better response for λ < 350 nm and worse response for λ > 900 nm when compared to that for HJT device resulting in lower value of integral current. Both PERC and HJT silicon solar cells provide high and close values of integral short circuit currents.

Average values of characteristics are presented in **Table 2**.

Dispersion values for the measured characteristics indicate rather good reproducibility of electronic properties observed in the device structures. For comparison, record data on HJT single wafer solar cell reported by "Kaneka Corp," Japan in 2017 [2]. This company increased its previous record in 2015 from PCE =25.1% to PCE = 26.6% in 2017 and the predicted efficiency exceeded 27% soon. It is worth to note that cells with record characteristics require
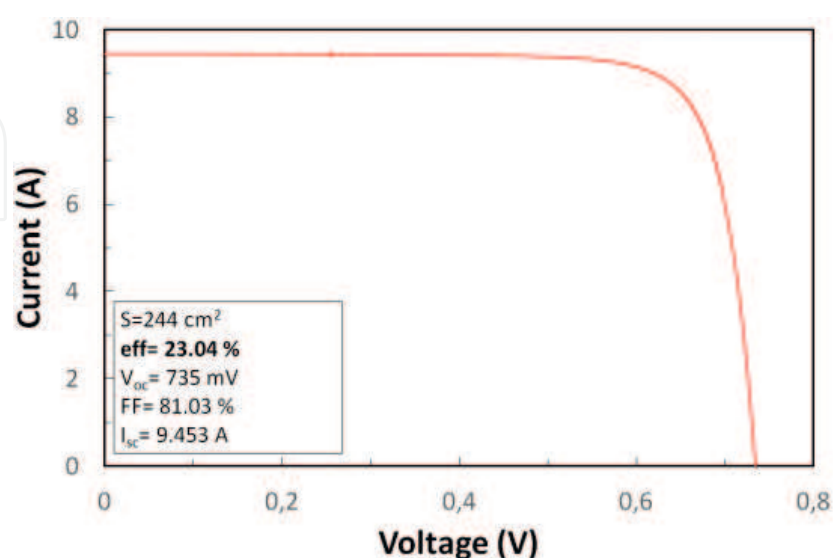

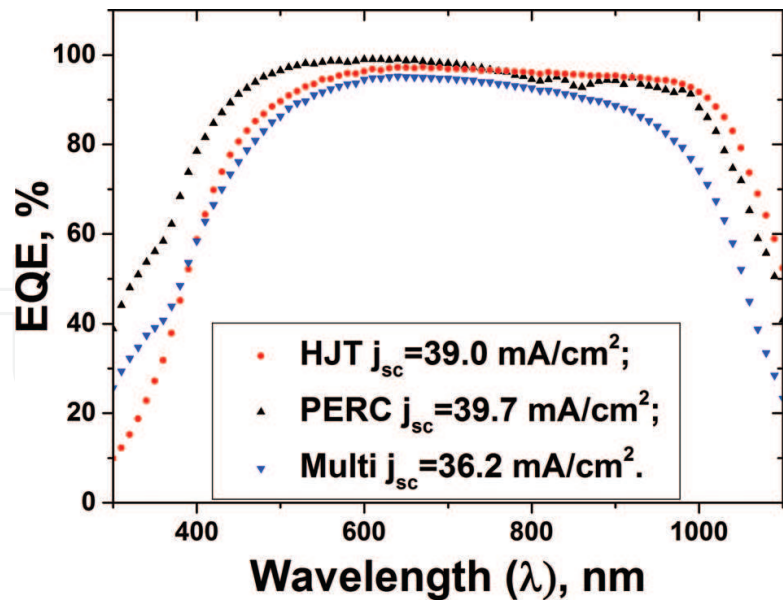**Figure 7.** Current-voltage I(U) graph and characteristics for single wafer HJT cell (156 × 156 mm^2).

Figure 8. Spectral response of PV cells fabricated with crystalline silicon, PECVD silicon films and combination in HJT structures.

	Isc (A)	Voc (V)	Pmax (W)	Vpmax (V)	Ipmax (A)	FF (%)	Eff (%)
Avg. value	9.45 ± 0.01	0.73 ± 0.01	5.52 ± 0.01	0.63 ± 0.01	8.80 ± 0.01	79.9 ± 0.1	22.6 ± 0.1
"Kaneka" 2017 [2]	10.37*	0.740	Not reported	Not reported	Not reported	84.7	26.6

*Calculation based on data in [2]: area S = 180 cm², density of short circuit current Jsc = 42.5 mA/cm².

Table 2. Performance characteristics of HJT single wafer (156 × 156 mm²) HJT solar cells.

usually special design and materials which may not be compatible with mass production conditions and/or facilities; however, such high efficiency level of laboratory cells demonstrates definitely potential for further improvement of HJT technology.

5. Implementation of the developed single wafer HJT structures in 1600 × 1000 mm² modules in industrial production

PECVD films for previous optimization were deposited in RDC TF TE laboratory system from "Oerlikon Solar," Switzerland, model Gen 5 KAI, photo is presented in **Figure 9(a)**. Reactor of this system is similar to the industrial system "KAI MT R1.0 Modular PECVD System" installed for industrial fabrication of the large modules S = 1600 × 1000 mm². Photo of this system is shown in **Figure 9(b)**. In both PECVD systems, capacitive glow discharge at frequency f = 40.68 MHz, is used, deposition temperature is about T_d = 200 C, technological gases of semiconductor purity.

(a)   (b)

Figure 9. Laboratory installation (a) and industrial PECVD system (b).

We shall skip description of technological process details and discuss only some specific issues related to HJT with crystalline silicon wafers large area module fabrication. Initially, these systems were employed for fabrication of thin film double junction tandem module on glass substrate (see diagram in **Figure 1(c)**). For HJT solar cell module, silicon wafers are placed on a special wafer carrier developed by RDC TF TE and then loaded into reactor. More details (process sequence, equipment, project milestones, etc.) on process of conversion silicon thin film solar module to high efficiency HJT module production can be found in ref. [11].

An important issue for large area modules is uniformity of electronic properties of the films deposited on large area substrate (or the carrier with 60 wafers).

Map of thicknesses for a-Si:H films deposited on large area glass substrate is shown in **Figure 10** with mean thickness value $<d> = 48.5$ nm and deviation of thickness $<\Delta d> = 7.1\%$. In other words, thickness of the films over entire reactor active area (1300×1000 mm^2) is better than 10%.

Figure 11 shows five-point average thicknesses and five-point bandgap values for the array of 5×5 silicon wafers, with mean values of thickness $<d> = 94.7$ and deviation 3.4% and with mean value of optical gap $<E_g> = 1.72$ eV and deviation $<\Delta E_g> = $HJT 1.1%. These characteristics meet uniformity requirement for fabrication of HJT cells on wafer distributed over entire reactor area with thin films incorporated in the device structure.

Performance characteristic of "Hevel" HJT solar cell module is shown in **Figure 12**. Comparison of this characteristic with that for HJT module reported by "Meyer-Burger" is presented in **Table 3**.

One can see in **Table 3** that the values reported by "Hevel Solar" are still less than those of "Meyer Burger." However, this difference partially comes from using full square wafers in MB modules, which results in reduced dead space area and corresponding gain in current value. It should be noted that it is difficult to perform correct comparison because of the difference in the form of silicon wafers (not always reported), in normalization over area taking
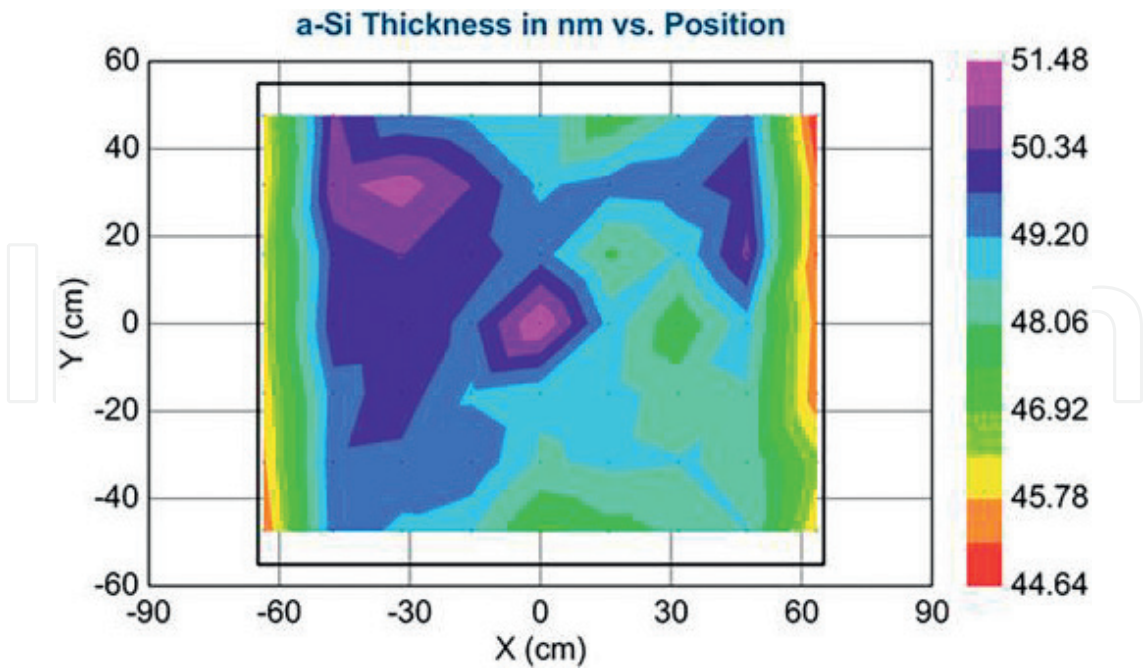
Figure 10. Thickness mapping for a-Si:H films deposited on glass substrate. Data are obtained by spectral ellipsometry.

into account substrate area occupied by contact grid or not, and so on resulting in some uncertainties when comparing the devices.

Interesting data on outdoor 1-year testing of "Hevel Solar" HJT modules can be found in Ref. [13] (**Figure 12**).
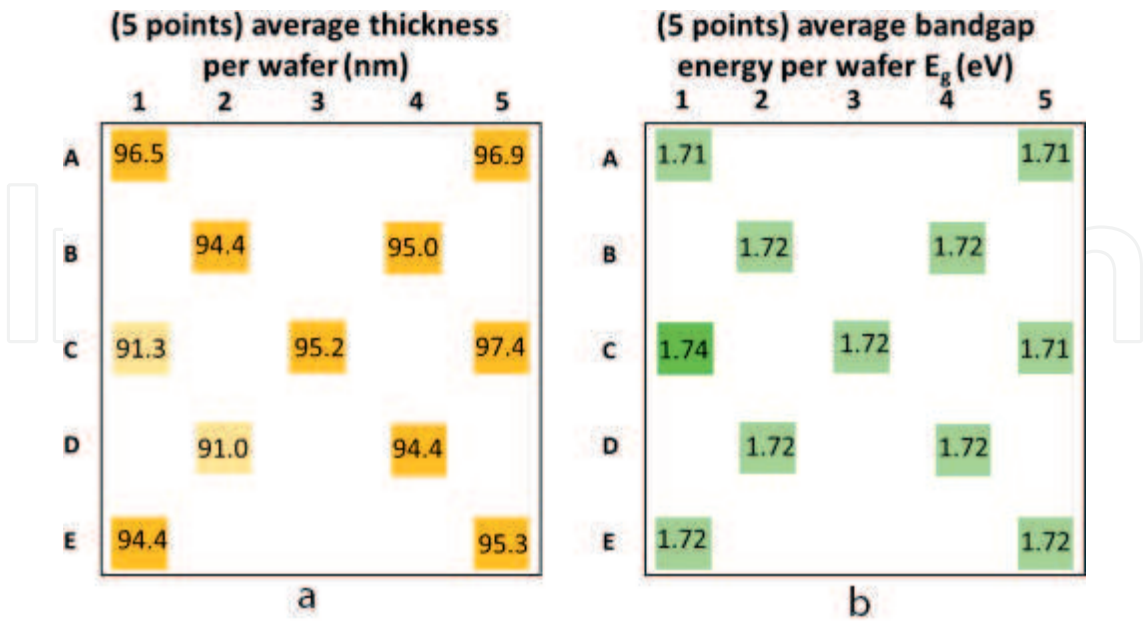

Figure 11. Thickness and optical gap mapping for the films deposited on silicon substrate (wafer dimensions 156 × 156 mm²). Data are obtained by spectral ellipsometry.

Module	Pmax	Vmp (V)	Imp (A)	Voc (V)	Jsc (A)	FF (%)	PCE (%)
"Hevel Solar"	317	35.78	8.85	43.88	9.44	76.4	19.1
"Meyer Burger"	329	37.04	8.89	44.28	9.66	77.0	19.8

Note: PCE indicated in table are effective values calculated with integral module area without subtraction area occupied by electrode stripes and elements of hermetization and assembling.

Table 3. Comparison of performance characteristics of 1600 × 1000 mm^2 HJT modules consisted of 60 single wafer cells made by "Hevel Solar" and "Meyer Burger" [12].

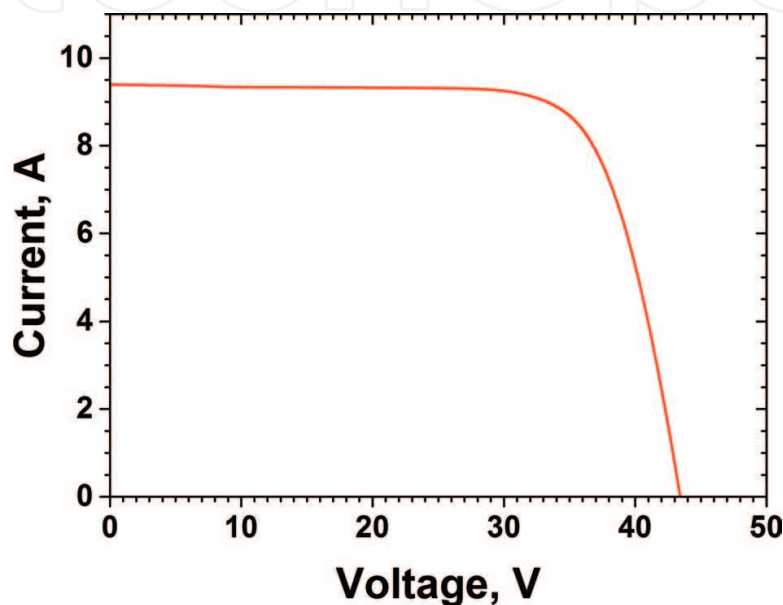**Figure 12.** Current-voltage I(U) characteristics of HJT module 1600 × 1000 mm^2 (60 cells 156 × 156 mm^2), developed by RDC TF TE and fabricated by "Hevel solar".

6. Summary and outlook

We have briefly described a successful transformation of technology for thin film solar cell modules (1000 × 1300 mm^2) with efficiency 11% to heterojunction technology (HJT) for c-Si solar cell modules (1000 × 1600 mm^2) with efficiency around 20% with employing the same essential equipment for PECVD materials. Now, the developed HJT modules are commercially produced by "Hevel Solar" (Russia) [14].

PECVD technique being principal in HJT module fabrication for both passivation and growth of semiconductor films is very versatile technology with high potential for further material engineering.

Well-known theoretical estimation of efficiency for one bandgap material c-Si gives value around PCE ≈ 30–34%, while record value achieved in 2017 by "Kaneka Corp." (Japan) is about PCE ≈ 27%. Thus some potential still exists for PCE increase for one gap c-Si HJT solar

cells, which can be realized by improving passivation, electrodes, improving short wavelength collection by frontal interface, and so on.

General road to increase conversion efficiency is related to multijunction (MJ) design and fabrication of PV structures comprising materials with different bandgaps adjusted for harvesting maximum of solar energy spectrum. This has been demonstrated by MJ solar cells with A_3B_5 semiconductors provided the highest reported values of PCE = 46% [15].

Therefore, MJ approach should be taken into account considering further development of HJT c-Si solar cells with efficiency above 34%.

Conflict of interest

Hereby the authors declare a lack of any known for them conflicts of interests.

Nomenclature

PECVD	plasma-enhanced chemical vapor deposition
ATR IR	attenuated total reflection infrared spectroscopy
FTIR	Fourier transform spectroscopy
HJT	heterojunction technology (devices, solar cells)
IBC	interdigitated back contact (solar cells)
PCE, η,	power conversion efficiency
E_g	optical gap, eV
PV	photovoltaic (structures, solar cells)
TCO	transparent conductive oxide
ITO	indium tin oxide
i-a-SiH	un-doped amorphous silicon
p-a-Si:H	p-doped amorphous silicon
n-a-Si:H	n-doped amorphous silicon
c-Si, (p)c-Si, (n)	c-Si un-doped crystalline silicon, p- and n-doped crystalline silicon
i-μc-SiH	un-doped microcrystalline silicon
n-μc-SiH	n-doped microcrystalline silicon
p-μc-SiH	p-doped microcrystalline silicon
p-SiC:H	p-doped microcrystalline silicon carbide

BSF	back surface field (solar cell)
CZ silicon	silicon fabricated by Czochralski technique
PERC	passivated emitter (usually p-Si) and rear cell (silicon solar cell).
PERL	passivated emitter rear locally diffused (silicon solar cell).
PERT	passivated emitter rear totally diffused (solar cells).
J_{sc}	short circuit current density, mA/cm^2.
I_{sc}	short circuit current, A
U_{oc}	open circuit voltage, V, mV
R_{sh}	effective shunt resistance, Ohm
R_s	effective series resistance, Ohm
STC	standard test conditions, output performance conditions used by most manufactures AM 1.5, I = 1000 W/m^2, T = 25°C
TMB	trimethyl boron

Author details

Eugenii Terukov[1], Andrey Kosarev[2]*, Alexey Abramov[1] and Eugenia Malchukova[3],

*Address all correspondence to: akosarev@inaoep.mx

1 R and D Center TFTE, Polytechnicheskaya, St-Petersburg, Russia

2 National Institute for Astrophysics, Optics and Electronics, Puebla, Mexico

3 Ioffe Institute, Polytechnicheskaya, St-Petersburg, Russia

References

[1] Int. Technology Roadmap for Photovoltaics, 2016 Results, 8th ed. September 8, 2017

[2] Yamamoto K, Yoshikawa K, Yoshida W, Irie T, Kawasaki H, Konishi K, Asatani T, Kanematsu M, Mishima R, Nakano K, Uzu H, Adachi D. High efficiency a-Si/c-Si heterojunction solar cells. In: Program Book, 27th International Conferece on Amorphous and Nanocrystalline Semiconductors, August 21-25, 2017, Seoul, Korea. p. 92

[3] Shah AV, Schade H, Vanecek M, Meier J, Vallat-Sauvain E, Wyrsch N, Kroll U, Droz C, Bailat J. Thin-film silicon solar cell technology. Progress in Photovoltaics: Research and Applications. 2004;**12**:113-142. DOI: 10.1002/pip.533

[4] Yang J, Banerjee A, Guha S. Triple junction amorphous silicon alloy solar cell with 14.6 initial and 13.0% stable conversion efficiencies. Applied Physics Letters. 1997;**70**:2975-2977

[5] Batzner DL, Habermann D, Andreeta L, Frammelsberger W, Kramer R, Lachenal D, Legradic B, Meixenberger J, Papet P, Strahm B, Wahli G. Heterojunction solar cells on p-type mono-Si wafers and the flexibility of HJT processing. In: Proceedings of 31rd European PV Solar Energy Conference and Exhibition. September 14-18, Hamburg, Germany. 2015. pp. 788-790. DOI: 10.4229/EUPVSEC20152015-2AV.3.33

[6] Release: Multicrystalline Silicon Solar Cell with 21.9 Repcent Efficiency: Fraunhofer ISE Again Holds World Record. February 20, 2017. pp. 1-3. Available from: https://www.ise.fraunhofer.de/content/dam/ise/en/documents/press-releases/2017/0617_ISE_e_PR_Weltrekord%20multi%20Si%20Solarzelle_final.pdf [Accessed: January 30, 2018]

[7] Masuko K, Shigematsu M, Hasiguchi T, Fujishima D, Kai M, Yoshimira N, Yamaguchi T, Ichihashi Y, Mishima T, Matsubara N, Yamanishi T, Takahama T, Taguchi M, Maruyama E, Okamoto S. Achievemnt of more than 25% conversion efficiency with crystalline silicon heterojunction solar cell. IEEE Journal of Photovoltaics. 2014;**2014**(11):1433-1435. DOI: 10.1109/JPHOTOV.2014.2352151

[8] Zhao J, Wang A, Altermatt A, Wenham PP, Green MA. 24% efficient PERL silicon solar cell: Recent improvements in high efficiency silicon cell research. Solar Energy Materials and Solar Cells. 1996;**41/42**:87-99

[9] Green MA, Blakers AW, Zhao J, Milne AM, Wang A, Dai X. Characterizzation of 23 percent efficient silicon solar cells. IEEE Transactions on Electron Devices. 1990;**37**(2):331-336

[10] Kherodia A, Panchal AK. Analysis of thickness-dependent optical parameters of a-Si:H/nc-Si:H multilayer thin films. Materials for Renewable and Sustainable Energy. 2017;**6**:23. DOI: 10.1007/s40243-017-0107-3

[11] Andronikov D, Abramov A, Abolmasov S, Emtsev K, Ivanov G, Nyapshaev I, Orekhov D, Semenov A, Shelopin G, Terukova E, Terukov E, Belkova N, Dubrovskiy A, Ishmuratov P, Ivanov A, Saykin D, Shakhray I, Smirnov A, Tarasov V, Timakov V, Tomchinskiy A, Kekelidze G. A successful conversion of silicon thin film solar cell module production to high efficiency heterojunction technology. In: Proceedings of 33rd European PV Solar Energy Conference and Exhibition, September 25-29, Amsterdam, Netherlands. 2017. pp. 732-735

[12] De Wolf S. High Efficiency Silicon Heterojunction Solar Cells: Properties, Processing, and Perspectives. Available from: http://www.icans26.org/icans26/EN/_SharedDocs/Downloads/EN/abstract%20de%20wolf.pdf?__blob=publicationFile [Accessed: Jan 29, 2018]

[13] Emtsev K, Malevsky D, Andronikov D, Abramov A, Yakovlev S, Titov A, Terukov E, Orekhov D, Bulygin B, Dubrovskiy A. Proceedings of 33-rd European PV Solar Energy Conference and Exhibition, September 25-29, 2017. Amsterdam, Netherlands. 2017. pp. 1628-1631

[14] Hevel achieves heterojunction cells with 22.8% efficiency as plant ramps. https://www.pv-tech.org/news/hevel-achieves-heterojunction-cells-with-22.8-efficiency-as-plant-ramps. [Accessed 2018- 01-29]

[15] Green MA, Hishikawa Y, Warta W, Dunlop ED, Levi DH, Hohl-Ebinger J, Ho-Baillie AWY. Progress in Photovoltatics: Research and Applications. 2017;**25**:668-676. DOI: 10.1002/pip.2909